Advanced Numerical Modelling of Footings on Granular Soils

P.K. Woodward[1], K. Nesnas[1] & D.V. Griffiths[2]

Abstract

Traditionally the analysis of footings on the surface of granular soils using finite elements has been difficult. This has generally led to a noticeable lack of published work in this area, especially for rough footings situated on the surface of granular soils with friction angles greater than 35°. The majority of published work has concentrated on the use of simple elastic perfectly plastic soil models, due to the computational difficulties and run times involved. In the present study a combined multi-surface isotropic & kinematic hardening model is used to study the behaviour of foundations on granular soils. The model gives a much more realistic account of material behaviour and therefore advances the state of the art in this area. The paper confirms the work of De Beer in which a reduction in $N\gamma$ was observed for increasing foundation widths. The paper highlights problems due to the development of singularities adjacent to the footing edge and confirms earlier work, using a simpler model, on the influence of the element depth under the footing on the computed bearing capacity. The paper concludes by presenting the allowable bearing pressures for three different sands as a function of the footing width.

Introduction

The bearing capacity of a foundation situated on the surface of a granular soil is usually determined by Terzaghi's equation

$$q_f = \frac{1}{2} s_\gamma \gamma B N_\gamma \qquad (1)$$

[1]Lecturer and Research Associate, Department of Civil & Offshore Engineering, Heriot-Watt University, Edinburgh, EH14 4AS, U.K.

[2]Professor of Engineering (Civil), Geomechanics Research Centre, Colorado School of Mines, Golden, Colorado, 80401-1887,U.S.A.

where, s_γ is a shape factor (equal to 1.0 for a strip footing and usually set to 0.6 for a circular footing), γ is the effective unit weight, B is the footing width or diameter and N_γ is the bearing capacity factor. This factor is usually determined by considering several different analytical formulae each giving a different value of N_γ, the friction angle ϕ is usually assumed to be constant. de Beer (1965) showed that N_γ is in fact a function of the foundation size, decreasing as the foundation width increased. The main reason for this decrease was explained through the dependence of the friction angle on the confining pressure (the larger the foundation, the larger the confining pressure at failure) and a grain size effect due to progressive failure. Yamaguchi *et al* (1976) showed that the grain size effect is only important beyond the peak. This suggests that localisation effects are only important once the peak resistance has been achieved, the nature of the post peak softening curve for the footing would then be dominated by the localisation. This means that the constitutive soil model used in the analysis would require a material length formulation to model post bifurcation behaviour.

Since it is only the peak resistance of the foundation that is of interest here, the main reduction in N_γ is therefore likely to be due to the pressure dependence of ϕ only. Hettler & Gudehus (1988) showed that the friction angle for a variety of sands of different initial densities varied by around 2 degrees in the pressure range 100-500 kPa. The majority of finite element analyses have been performed using simple elastic perfectly plastic Mohr-Coulomb constitutive soil models. These types of models do not realistically simulate the real observed behaviour of granular foundations as they do not simulate the deformation or strength characteristics of the soil very well. Recent attempts to compute N_γ using simple models have been performed by Griffiths (1982), Simonini (1993), Manoharan & Dasgupta (1995) and Frydman & Burd (1997). Woodward & Griffiths (1998) showed that any reductions in N_γ computed using these simple models was due to mesh effects and that its absolute value was related to the depth of the first row of contact elements when a 'uniform' mesh was used. By using a simple technique, they showed how lower values of N_γ could be obtained, which tended towards 'analytical' solutions as the element depth reduced.

It has been suggested that more accurate values of N_γ can be obtained when the element adjacent to the footing is refined. The work presented in this paper shows however that fixing the corner element can still lead to difficulties in mesh dependency when the first element depth is varied. If the foundation width is to be investigated, one must ask what size must the corner element be for a given foundation roughness, size and shape? Woodward & Griffiths (1998) suggested that one should try to use B/d>=10 for uniform meshes to overcome mesh dependency problems, where d=depth of the first row of elements under the contact nodes. The B/d ratio should also be kept constant when the footing width is varied. If refinement is to be used in favour of a uniform mesh, then adaptive mesh refinement would seem to be the next logical step to overcome problems associated with the refinement of a single element. This approach may also help to overcome localisation problems.

The principal reason why Woodward & Griffiths (1998) were unable to directly compute the analytical value of N_γ (for an idealised foundation, as given by Bolton & Lau, 1993) was due to no correction being applied due to the development of singularities. The work present here clearly shows these singularities developing at the Gauss points adjacent to the footing edge as deformation increases. The real value of N_γ, for a given foundation, is a function of the stress-strain characteristics of the soil. For example, its value is not only a function of the mean stress, but also the dilatancy properties, increasing with dilatancy angle. It is therefore essential that realistic soil models are used, calibrated to real soil behaviour. In this work an advanced multi-surface kinematic soil model is used as it accurately simulates the observed stress-strain behaviour of granular soils.

Although the computation of N_γ is of importance in foundation design, the primary concern is still settlement behaviour. The simple models applied to date in granular foundation studies cannot simulate settlement behaviour very well and so advanced models must be used if the state of the art is to be pushed forward. Realistic simulation of soil allows the computation of the allowable bearing pressures used in general design to be determined. The allowable pressure often represents the bearing pressure at 0.04m settlement and is investigated here for the soils considered.

Constitutive Soil Model ALTERNAT

Often advanced soil models are only used to demonstrate the simulation of triaxial stress paths. One can only assume that these models are not yet implemented into a more useful general purpose finite element program. In this paper, the elasto-plastic multi-surface kinematic constitutive soil model ALTERNAT (Molenkamp, 1982, 1990) is used. This model has been shown to be able to analyse a wide range of problems involving differing stress paths (Molenkamp 1990, Woodward, 1993), including granular foundation behaviour (Nesnas & Woodward, 1999 and Woodward & Molenkamp, 1999). The model can simulate both the monotonic and cyclic behaviour of granular soils. For the purposes of this paper only the most salient features of the model for monotonic footing analysis are included.

The following effective stress invariants are used in the outline description of the model. The isotropic stress s and the isotropic strain v respectively can be calculated from the following expressions

$$s = \frac{1}{\sqrt{3}}\sigma_{ij}\delta_{ij} \quad \text{and} \quad v = \frac{1}{\sqrt{3}}\varepsilon_{ij}\delta_{ij} \tag{2}$$

where, σ_{ij} is the Cauchy stress, ε_{ij} is the strain and δ_{ij} is the Kronecker delta. The deviatoric stress t and the deviatoric strain e can be obtained from the following expressions

$$t = \sqrt{(t_{ij}t_{ij})} \quad \text{and} \quad e = \sqrt{(e_{ij}e_{ij})} \tag{3}$$

where, t_{ij} is the deviatoric stress tensor and e_{ij} is the deviatoric strain tensor. In ALTERNAT the plastic properties are calculated in the co-rotational frame, which means that they are determined with respect to a set of axes that rotate with the material during deformation. The non-linear elastic component of the model is based on the following complementary potential function Q after Molenkamp (1992)

$$Q = A\frac{p_a}{(P+1)}\left(\frac{s}{p_a}\right)^{P+1}\left[1+\frac{3P(P+1)}{4R}\left(\frac{t}{s}\right)^2\right] \tag{4}$$

where, the scalars A, P and R are the elastic material parameters and p_a is the atmospheric pressure (assumed to be 100 kPa). The inverse of the elastic tangent stiffness matrix D^{-1}_{ijkl} is the second order partial derivative of equation (4).

To simulate the initial anisotropy of the soil, or to simulate stress-induced anisotropy during loading, the yield surface is centred around a non-zero deviatoric stress state when viewed in the deviatoric plane. A pseudo stress T_{ij} is now used to represent the mobilised friction

$$T_{ij} = \sigma_{ij} - \frac{1}{3}\sigma_{kl}\delta_{kl}\xi_{ij} \tag{5}$$

where, σ_{ij} is the 'active' stress and ξ_{ij} is a non-dimensional deviatoric tensor of anisotropy. The hardening modulus (or plastic stiffness) of the soil changes as the yield surfaces expands and moves in the deviatoric plane. The shape of the yield surface is given by the Lade & Duncan (1975) and Lade (1977) smooth conical surface

$$F\left[I(T_{ij})\right] - f(\chi) = \frac{I_1^3}{I_3} - 27 - f(\chi) = 0 \tag{6}$$

where, χ is the hardening parameter and $f(\chi)$ is the size of the yield surface. I_1 and I_3 are the first and third invariants of the pseudo-stress respectively.

The plastic stiffness of the soil it determined through the hardening modulus H. The hardening modulus is related to the pre-peak strain hardening and post-peak strain softening behaviour of the soil. For isotropic hardening, the hardening modulus H is found from the following equation

$$H = \frac{df}{d\left(\frac{t}{s}\right)} \frac{d\left(\frac{t}{s}\right)}{d\chi} f\left(n_i, \Sigma\Delta\varepsilon^p_{vol,c}, \chi, \frac{s}{p_a}\right) \tag{7}$$

where,

$$\frac{df}{d\left(\frac{t}{s}\right)} = 81 \frac{\left(\frac{t}{s}\right)}{\left[1+\sqrt{2}\left(\frac{t}{s}\right)\right]^2 \left[1-\frac{1}{\sqrt{2}}\left(\frac{t}{s}\right)\right]^3} \tag{8}$$

This expression is determined by rearranging equation (6) and substituting for the stress invariants I_1 and I_3 by the shear stress level $\left(\frac{t}{s}\right)$ for triaxial compression.

The $\frac{d\left(\frac{t}{s}\right)}{d\chi}$ component of equation (7) is obtained by considering the strain hardening and softening behaviour of the material and differentiating with respect to the hardening parameter. If the pre-peak straining hardening shear stress level is Y_1 and the post-peak shear stress level is Y_2 a smooth transition from Y_1 to Y_2 is given by

$$\left(\frac{t}{s}\right) = \frac{Y_1 Y_2}{\left(Y_1^n + Y_2^n\right)^{\frac{1}{n}}} \tag{9}$$

where, n is a material parameter and can be chosen to ensure that the correct peak shear stress level is observed. The function at the latter part of equation (7) is used to simulate cyclic densification using the porosity n_i, the accumulated plastic volumetric strain $\Sigma_c \Delta\varepsilon^p_{vol,c}$, the hardening parameter χ and the isotropic stress level $\frac{s}{p_a}$. Y_1 and Y_2 are obtained from the following

$$Y_1 = \left[\frac{e^p}{\left(\frac{s}{p_a}\right)^L \frac{(1+e_v)E}{(Q-e_v)^2}}\right]^{\frac{1}{D}} \tag{10}$$

$$Y_2 = M\left\{(1-\upsilon) + \upsilon.\exp\left(-\psi\left(\frac{s}{p_a}\right)\right)\right\}\exp\left(-\beta e_v\right) \tag{11}$$

where, E, Q and D are the pre-peak strain hardening parameters and M, υ, ψ and β are the post-peak strain softening parameters. The pre-peak strain hardening and post peak strain softening shear stress levels are therefore related to the mean isotropic stress level (s/p_a), the void ratio e_v and the plastic deviatoric strain e^p. This will

obviously have a significant effect when looking at the reduction in N_γ with footing width (the larger the footing width, the higher the mean stress at failure).

In ALTERNAT, the direction of the plastic strain increment is first decomposed into an isotropic and a deviatoric component. The isotropic component $\alpha\delta_{ij}$ is based on Rowe's stress-dilatancy theory (1962, 1971) for granular soils and is obtained from the plastic dilatancy ratio.

$$d\varepsilon_{ij}^{p} = \frac{\partial G}{\partial \sigma_{ij}}\lambda = \left(\alpha\delta_{ij} + \frac{\partial G^{d}}{\partial \sigma_{ij}}\right)\lambda \quad \text{where} \quad \frac{dv^{p}}{de^{p}} = \alpha\sqrt{3} \tag{12}$$

Molenkamp (1982, 1990) has developed several expressions to determine the plastic dilatancy ratio for loading/ unloading in triaxial compression and extension. A function is then used to look at other Lode angles. The characteristic shear stress level $\left(\frac{t}{s}\right)_{\mu c}$ at zero dilatancy is obtained from the true interparticle friction angle ϕ_μ, using the following

$$\left(\frac{t}{s}\right)_{\mu c} = C\left[(1+\xi) - \xi\exp\left(-\theta_p\left(\frac{s}{p_a}\right)\right)\right]\left[1-\exp(-\varsigma e_v)\right] \tag{13}$$

where, C, ξ, ζ and θ_p are material parameters. As the isotropic stress increases the shear stress level at which dilation will occur also increases, simulating the reduction in dilation with high confining pressures. This is an important characteristic in foundation problems since N_γ is strongly dependant on the dilatancy angle of the soil.

The deviatoric component of the plastic potential $\left(\frac{\partial G^{d}}{\partial \sigma_{ij}}\right)$ is based on the expression used to determine the yield function, except that a reduced modified pseudo-stress T^{*} is used to make the deviatoric potential surface more circular in the deviatoric plane.

The critical state of the model is formed by equating the post-peak shear stress level (equation 11) to the shear-stress level at zero dilatancy (equation 13) to give

$$\exp(-\beta e_v) = \left[M\left\{(1-\upsilon)+\upsilon\exp\left(-\psi\left(\frac{s_c}{p_a}\right)\right)\right\} + C\left\{(1+\xi)-\xi\exp\left(-\theta_p\left(\frac{s_c}{p_a}\right)\right)\right\}\right]^{-1} \cdot C\left\{(1+\xi)-\xi\exp\left(-\theta_p\left(\frac{s_c}{p_a}\right)\right)\right\} \tag{14}$$

The void ratio at the critical state of the material is therefore dependant on the post-peak strain softening parameters, the true interparticle friction angle parameters and the isotropic stress level at the critical state $\left(\frac{s_c}{p_a}\right)$. In total there are 24 material parameters associated with the model, however only 6 parameters are required to be determined from triaxial compression tests for monotonic loading, the remainder can be considered as constant. The current capabilities of the model are: non-linear elasticity; pre-peak strain hardening; post-peak strain softening; dilatancy based on Rowe's stress-dilatancy theory; critical state; cyclic mobility and densification; tensile strength. The cyclic capabilities of the model are not used in the present work.

The material parameters used in the calibration of the model to the different sands used in this study (Hostun γ=16.30 kN/m^3, Nevada γ=15.14 kN/m^3 & Ersak γ=16.25 kN/m^3) can be found in Nesnas & Woodward (1999) and Woodward & Molenkamp (1999). However, an example of the calibration of the model to Nevada sand is shown in Figure 1. Here, the model is calibrated to the sand at a relative density of D_r=40% (γ=15.14 kN/m^3) at confining pressures of σ_c=40,80 and 160 kPa.

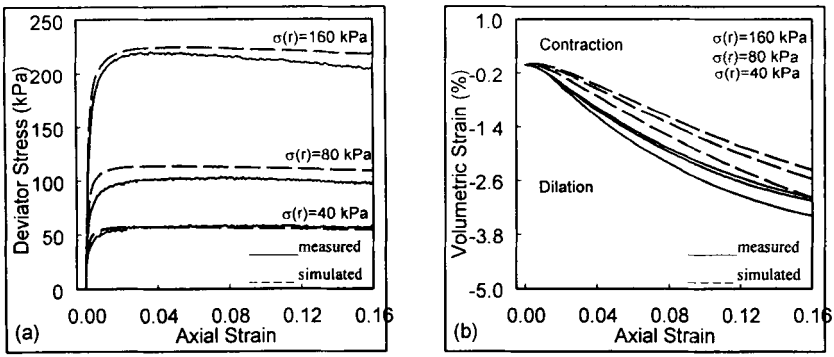

Figure 1 Calibration of ALTERNAT to Nevada sand at γ=15.14kN/m^3

Computer Program FALTICA

In general, the first author has termed the finite element program used in this paper FALTICA (Footing ALTernat Incremental Computer Algorithm). The program uses 8-noded quadrilateral finite elements and a 2x2 integration rule (Smith & Griffiths, 1988 & 1998). A constant stiffness matrix is adopted as the reference and an iterative procedure is used to correct the unbalanced plastic forces with a note kept on which yield surface is currently active for stress redistribution.

The bearing stress at failure is calculated using three different methods. The first

method (termed *q_avg*) simply averages the vertical component of the Gauss point stresses (σ_y) directly under the footing

$$q\_avg = \frac{\sum_{1}^{2n} R \times \sigma_y}{2n} \tag{15}$$

where, n is the number of direct contact elements and R is the element stress scaling factor for axi-symmetry / plane strain. The second method (termed *q_bts*) determines the equivalent vertical nodal forces for the direct contact elements only

$$q\_bts = \frac{\sum_{1}^{n} F_y \left\{ \iint \left(B^T \sigma \right) dx dy \right\}}{\text{Footing Area}} \tag{16}$$

where, B^T=transpose of the strain-displacement matrix. The third method (termed *q_bts_o*) determines the equivalent vertical nodal forces for the direct contact elements and includes contributions from the adjacent elements next to the footing

$$q\_bts\_o = \frac{\sum_{1}^{m} F_y \left\{ \iint \left(B^T \sigma \right) dx dy \right\}}{\text{Footing Area}} \tag{17}$$

Where, m is the number of surface elements. A correction for the initial surcharge is made in all three methods.

Finite Element Analysis

Figure 2 shows the mesh used in the analysis. The footing is assumed to be rigid and circular or strip in cross section. The interface between the footing and the soil is assumed to be perfectly rough and the footing is subjected to equal displacement increments applied to the vertical degrees of freedom at the contact nodes (restraining the horizontal degrees of freedom at the contact nodes simulates the rough condition). The rough analysis is used to demonstrate the robustness of the finite element implementation.

The footing widths/diameters considered were B=1m to 6m. The procedure proposed by Woodward & Griffiths (1998) was used to determine the first element depth for all footing sizes. The mesh size is $10B$ x $10B$ and the mesh boundary conditions are; fully restrained at the base of the mesh and free vertical movement only along the sides. The initial vertical stress is set by multiplying the vertical distance of the Gauss point from the surface of the sand by the unit weight γ of the soil The horizontal stresses are then set by multiplying the vertical stresses by the

earth pressure at rest coefficient K_o. It was found that the value K_o did not significantly influence the results and so was set at K_o=1 for convenience.

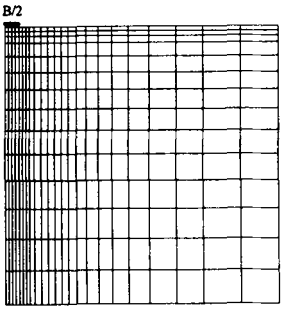

Figure 2 Mesh used in footing studies

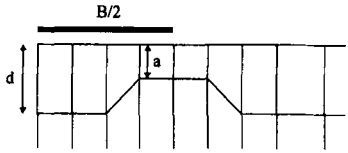

Figure 3 Refinement of the corner element

It has been suggested that the size of the corner element adjacent to the footing has an effect on the behaviour of the foundation (e.g. Figure 3). This is not surprising due to the development of the singularities shown below. However, attempting to determine what the size of this element should be for different foundation widths, roughness values, constitutive model, finite element shape, as well as dilatancy properties and friction angles of the soil, would prove too cumbersome. This is demonstrated in Figure 4, where the corner element for a 2m rough strip footing on Nevada sand is fixed at a=0.25m and the remainder of the contact element depths increased. A dependence on the B/d ratio still exists, this suggests that we must keep reducing the corner element size for a given foundation width to obtain consistent results.

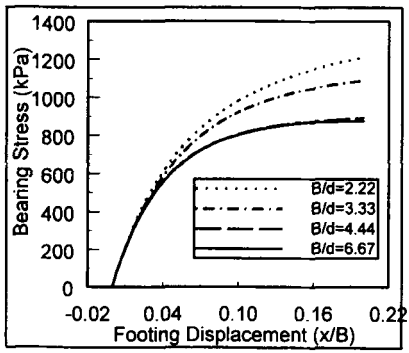

Figure 4 Effect of the corner element on the footing response

The suggestion of setting B/d>=10 for a uniform mesh (to get consistent results) would therefore appear to be more appealing than trying to adjust both the corner element and the remainder of the contact elements' depth (it is also more practical in many cases).

Frydman & Burd (1997) commented that the singularity at the footing edge could increase the computed value of N_γ. They suggested correcting the pressure distribution under the footing by the computed edge stress. In a real soil, the development of this singularity does not first occur at the footing edge however, but a small distance away from it. This can clearly be seen in Figure 5, with the occurrence of the first singularity at position 3. After some initial strain hardening, the stress path follows the failure surface back towards the origin (i.e. zero isotropic stress) generating the singularity. In this particular case, it was observed that the ratio of bearing stress q to bearing capacity q_f, was q/q_f=20% when this first singularity occurred.

In FALTICA, all plastic stresses (co-rotational) are redistributed once a pre-defined isotropic stress has been reached. This enables the correct pressure distribution to be simulated underneath and adjacent to the foundation, by ensuring no further increases in shear capacity. The correction can be thought of as a sophisticated no-tension type of correction. Since the velocity of the elements adjacent to the foundation is upward (the soil is dilating) there can be no contribution of the singular Gauss points to the shear strength of the foundation. This means that equations (16) & (17) will give the same value at failure. In fact, Figure 6 shows that equations (15)-(17) all give the value of the bearing capacity at failure.

Variation of N_γ with Footing Width

Figure 7 shows the predicted reduction in the peak friction angle with confining pressure for Huston, Nevada & Ersak sand. The reduction is of the order of 1.74 degrees over the 100-500kPa pressure range. This is close to the reduction as observed by Hettler & Gudehus (1988). Typical values of the friction angle in triaxial compression for the three sands considered are ϕ=36.7°, ϕ=34.2°, ϕ=33.6°, for Huston, Nevada & Ersak sands respectively, at a confining pressure of σ_c=300 kPa.

Figure 8 shows the results of finite element simulations for rough circular footings on the surface of the three sands considered, for B=1 to 6m. The results are presented in terms of normalised average pressure $2q/\gamma B$ beneath the base of the footing (equation (15)). It should be noted that the values presented are not normalised with respect to a foundation 'shape' factor. The figure clearly shows that the bearing capacity factor N_γ decreases with increasing footing width due to the pressure dependence of ϕ and tends towards a constant value as B increases. As commented earlier, a reduction in the dilation angle with increasing confining

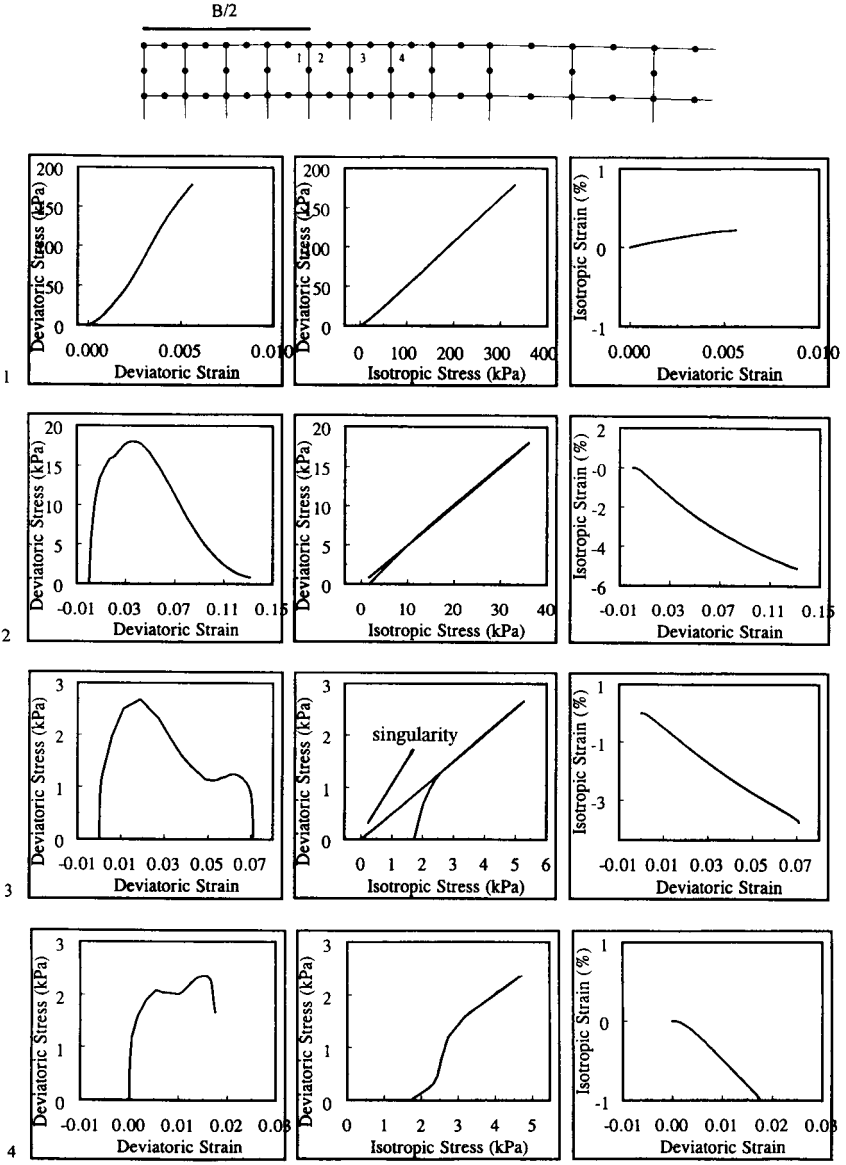

Figure 5 Development of singularities adjacent to the footing edge

pressure is also simulated. This will also contribute to the reduction in N_γ with increasing footing width.

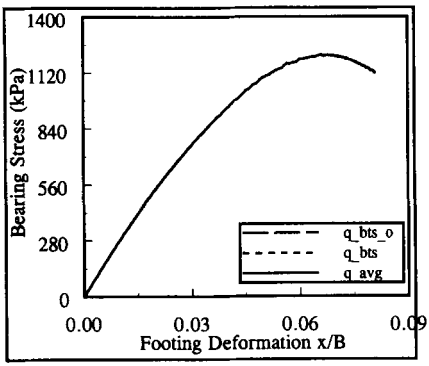

Figure 6 Effect of calculation method on footing response

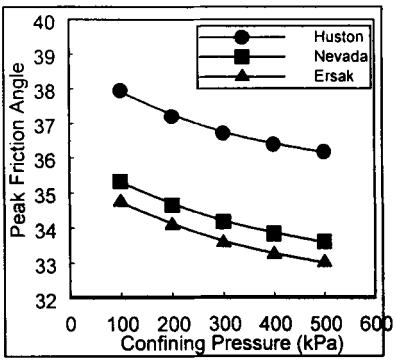

Figure 7 Reduction in the peak friction angle with confining pressure

The allowable bearing pressure for an isolated footing is often defined as the value of the pressure at which a settlement of 0.04m occurs. Although other settlement values have been proposed in the literature, this value is used here to determine the allowable bearing pressure.

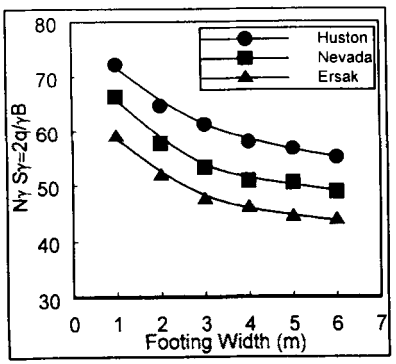

Figure 8 Reduction in bearing capacity $N_\gamma S_\gamma$ with footing width for a rough circular footing

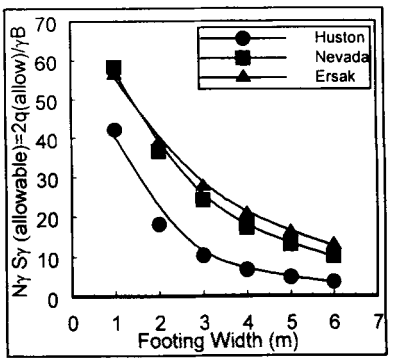

Figure 9 Reduction in allowable bearing capacity $N_\gamma S_\gamma$ (allowable) with footing width for a rough circular footing

Figure 9 shows the variation of the allowable pressure (again normalised to $N_\gamma S_\gamma$) with footing width for the three sands considered. As expected, the allowable pressure decreases with footing width. In fact, the authors have found that the allowable bearing pressure varies with footing roughness, shape, and size as well as the soil type. Although not considered here, an overall allowable bearing pressure could be determined by considering the factor of safety of each footing width as well as the computed settlement response.

Conclusions

The footing width B to first element depth d ratio (B/d) has an effect on the computed bearing capacity of a footing on the surface of granular soil. For a uniform mesh, this effect can be minimised using values of $B/d>=10$ (in fact values of $B/d>=7$ have been found in this work to provide sufficiently accurate values of N_γ). The singularity developed at the footing edge can influence the bearing capacity of the foundation and must be accounted for. The computer program FALTICA was shown to be able to simulate the decrease in the bearing capacity factor N_γ with increasing foundation width. This is due to the simulated reduction in peak friction angle and dilatancy properties with increasing confining pressure.

The allowable bearing pressure also reduces as the footing width increases. This reduction is related to the footing size, roughness and shape as well as the soil's stress-strain characteristics. It would seem that accurate simulations of granular foundation behaviour using finite elements can only be achieved when more realistic constitutive soil models are used.

Acknowledgements

The authors gratefully acknowledge the support of the Engineering and Physical Science Research Council, UK (grant reference number GR/L75498).

References

de Beer, E.E. (1965) "Bearing Capacity and Settlement of Shallow Foundation on Sand", *Proc. Symp Bearing Capacity and settlements of foundations*, Duke University, 15-33.

Bolton, M.D. & Lau, C.K. (1993) "Vertical bearing capacity factors for circular and strip footings on Mohr-Coulomb soil". *Canadian Geotechnical Journal*, Ottawa, Canada, 30(4),1024-1033.

Frydman, S. & Burd, H.J. (1997) "Numerical studies of bearing capacity factor N_γ", *J. Geo. Eng., ASCE*, Vol 123, No. 1, 20-29.

Griffiths, D.V. (1982) "Computation of bearing capacity factors using finite elements", *Geotechnique*, 32, (3), 195-202.

Hettler, A. and Gudehus, G., (1988) "Influence of the Foundation Width on the Bearing Capacity Factor", *Soil and Fdns, Jap. Soil Mech. Fdns. Eng.* 28, No. 4, 81-92.

Lade, P.V. & Duncan, J.M. (1975) "Elasto-plastic stress-strain theory for cohesionless soils", *J. Geotech. Eng. Div. ASCE.* 107, GT10, 1037-1053.

Lade, P.V. (1977) "Elasto-plastic stress strain theory for cohesionless soil with curved yield surfaces", *Int J. Solids Struct.* 13, 1019-1035.

Manoharan, N. & Dasgupta, S.P. (1995) "Bearing capacity of surface footings by finite elements", *Comp. Struct*, 54, No.4, 563-586.

Molenkamp, F. (1982) "Kinematic model for alternating loading ALTERNAT", *LGM Report CO-218598*, Delft Geotechnics.

Molenkamp, F. (1990) "Reformulation of ALTERNAT to minimise numerical drift due to cyclic loading", *Internal Report*, University of Manchester.

Molenkamp, F. (1992) "Application of non-linear elastic model", *Int. J. for Numer & Analyt. Methods. in Geomech.*, Vol 16, 131-150.

Nesnas, K. & Woodward, P.K. (1999) "Advanced bearing capacity computation of a footing on sand using a kinematic hardening elasto-plastic model" *Proc. NUMOG VII Conf.*, Austria, 463-468.

Rowe, P.W. (1962) "The stress-dilatancy relation for static equilibrium of an assembly of particles in contact", *Proc. Royal Soc.*, Vol. 269, 500-527.

Rowe, P.W. (1971) "Theoretical meaning and observed values of deformation parameters for soil", *Proc. Roscoe Mem. Symp.*, Cambridge, 143-194.

Simonini, P. (1993) 'Influence of relative density and stress level on the bearing capacity of sands', *Int. J. for Numer.& Analyt. Methods. in Geomech.*, Vol. 17, 871-890.

Smith, I.M. & Griffiths, D.V. (1988) "Programming the finite element method", John Wiley & Sons, 2nd Edition.

Smith, I.M. & Griffiths, D.V. (1998) "Programming the finite element method", John Wiley & Sons, 3rd Edition.

Woodward, P.K. (1993) "Earthquake engineering and advanced constitutive modeling in geomechanics, by finite element", *PhD Thesis*, University of Manchester.

Woodward, P.K. & Griffiths, D.V. (1998) "Observations on the computation of the bearing capacity factor N_γ by finite elements", *Geotechnique* 48, No. 1, 137-141.

Woodward, P.K. & Molenkamp, F. (1999) "Application of an advanced mult-surface kinematic soil model", *Int. J. for Numer. & Analyt. Methods. in Geomech.* Vol. 23, 1995-2043.

Yamaguchi, H. Kimura, T. & Fuji, N. (1976) "On the influence of progressive failure on the bearing capacity of shallow foundations in dense sand". *Soil & Foundations*, 16, No.4 11-22.